Selenium Adsorption on Au(111) and Ag(111) Surfaces: Adsorbed Selenium and Selenide Films

ARTICLE *in* THE JOURNAL OF PHYSICAL CHEMISTRY C · APRIL 2013

Impact Factor: 4.77 · DOI: 10.1021/jp4007203

THE JOURNAL OF PHYSICAL CHEMISTRY C

Article

pubs.acs.org/JPCC

Selenium Adsorption on Au(111) and Ag(111) Surfaces: Adsorbed Selenium and Selenide Films

Juanjuan Jia,[†,‡] Azzedine Bendounan,[§] Harish Makri Nimbegondi Kotresh,[∥] Karine Chaouchi,[§] Fausto Sirotti,[§] Srinivasan Sampath,[∥] and Vladimir A. Esaulov*[,†,‡]

[†]Institut des Sciences Moléculaires d'Orsay, Université-Paris Sud, Orsay, France

[‡]CNRS, UMR 8214, Institut des Sciences Moléculaires d'Orsay, Bâtiment 351, Université-Paris Sud, 91405 Orsay, France

[§]Synchrotron SOLEIL, L'Orme des Merisiers, Saint-Aubin, BP 48, F-91192 Gif-sur-Yvette Cedex, France

[∥]Department of Physical and Inorganic Chemistry, Indian Institute of Science, Bangalore, India

Supporting Information

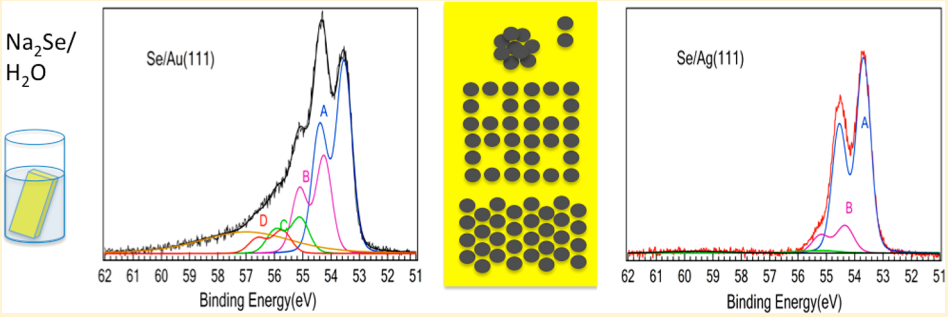

ABSTRACT: Results of a high resolution photoemission and electrochemistry study of Se adsorption on Au(111) and Ag(111) surfaces performed by immersion of pristine samples into an aqeuous solution of Na_2Se are presented. Cyclic voltammetry on Au shows formation of selenium adsorbed species and the structures observed in reductive desorption are related to the atomic and polymeric species observed in XPS. In the case of Au(111) XPS spectra in the Se(3d) region indeed show two main features attributed to Se chemisorbed atomically and polymeric Se_8 features. Smaller structures due to other types of Se conformations were also observed. The Au(4f) peak line shape does not show core level shifts indicative of Au selenide formation. In the case of silver, XPS spectra for the Ag(3d) show a broadening of the peak and a deconvolution into Ag_B bulk like and Ag_{Se} components shows that the Ag_{Se} is located at a lower binding energy, an effect similar to oxidation and sulfidation of Ag. The Se(3d) XPS spectrum is found to be substantially different from the Au case and dominated by atomic type Se due to the selenide, though a smaller intensity Se structure at an energy similar to the Se_8 structure for Au is also observed. Changes in the valence band region related to Se adsorption are reported.

INTRODUCTION

Adsorption of chalcogen atoms on surfaces is attracting attention in recent years in relation to self-assembly of organic molecules bearing chalcogen atom head groups as linkers and in the context of creation of novel interfaces and nanostructures. Thus, in recent years adsorption of sulfur on gold and other surfaces has been the focus of renewed attention in relation with questions of self-assembly of organic molecules and formation of self-assembled monolayers (SAMs) such as alkane and aromatic thiols[1−6] and dithiols.[3,7−11] The alkanethiol−metal and alkanethiol−alkanethiol interactions are not fully understood. These interactions determine the stability of SAMs, a crucial point for their use in many technological applications. There has been progress in the understanding of the lateral interactions prevailing in SAMs, but the nature of the S−Au bond is not fully understood.[12−15] In fact, although the chemical state of S atoms at the alkanethiol/Au interface has been extensively studied by XPS, the interpretation of experimental data still remains controversial and is the object of ongoing research.[12] There are also indications that the S−Au bond in alkanethiol adlayers differs from the S−Au bond in S lattices. Several recent works have therefore focused on aspects of sulfur atom chemisorption.[12,13,16−18]

Work on adsorption of the heavier chalcogenide atoms and SAMs is not extensive. Selenium and tellurium derived SAMs have attracted interest[19−26] as alternatives to thiol-derived SAMs, in, for example, molecular electronics applications, because of different (Se as compared to S) bonding to the substrate: this is a point of key importance for electronic transport. Recent experiments on assembly of alkaneselenides[21,25] from liquids, more than one adsorption states is

Received: January 22, 2013
Revised: April 17, 2013
Published: April 18, 2013

   dx.doi.org/10.1021/jp4007203 | J. Phys. Chem. C 2013, 117, 9835−9842

evidenced by core-level shift analysis of high resolution XPS and also experiments show a large diversity in molecular arrangements at intermediate coverages. It has also been suggested that dissociative adsorption could occur in some cases, resulting in appearance of atomic Se on the surface.[26]

Studies of Se and Te adsorption are much more rare than those of S.[27−40] A few studies of Se adsorption on Au and Ag surfaces have been reported in electrochemical studies starting from selenium oxides.[32−34] Some of these were performed in conjunction with tunneling microscopy and on Au showed the existence[33] of chemisorbed Se and square ring structures attributed to Se_8 molecules. This is similar to the case of S.[15,17] Some other dimer, trimer, and chain-like Se structures were also observed.[33] In the case of Ag,[34] Se layers formed by bulk Se electrodeposition followed by stripping of the loosely bound bulk Se, showed ordered structures that are very different from those on Au(111) and exhibiting a low adatom density.

A thorough spectroscopic characterization of the Se−gold and −silver interfaces is still missing and would be a useful complement to current investigations on self-assembly. Besides this interest, it is worth mentioning that selenides,[37−43] for example, bulk silver selenide,[37,39,42,43] have attracted interest because of various applications as a photosensitizer in photography, in photochargeable batteries, and as a thermoelectric material[38] and also it has been found that nonstoichiometric silver selenide displays giant magnetoresistance.[41] These features have stimulated recent interest in studies of Ag_2Se films,[37] nanocrystals, and nanotubes.[40]

In this work our objective was to obtain spectroscopic information on binding energies and valence band characteristics and explore an easy way of creating an Se chemisorbed layer by immersion of gold and silver samples into aqueous solutions of Na_2Se, which serves as a Se source,[44,45] by analogy with what has been done for sulfur.[15,17] In this paper we report results of XPS measurements, including a valence band study and also a cyclic voltammetry study of Se on Au.

EXPERIMENTAL SECTION

Substrates. In the photoemission experiments, monocrystalline samples of Au(111) and Ag(111) were used and the preparation involved multiple cycles of sputtering and annealing. Crystallinity and cleanliness were checked by LEED and by XPS and characteristics of the valence band photoemission by scanning in the 0−800 eV photon energy range.

For the electrochemistry measurements we used gold on glass samples that were cleaned in a 5:1:1 mixture of deionized (Milli-Q) water, 25% hydrogen peroxide, and 30% ammonia following a procedure outlined in ref 46. As noted previously,[7−9] these substrates are well suited for self-assembly experiments and present large Au(111) terraces.

Se Adsorption. The selenium adsorption was made by immersing clean samples into a 3 millimolar Na_2Se solution in a 0.1 molar NaOH aqeuous solution. Na_2Se was purchased from Alfa Aesar and used as received. Na_2Se was stored in an Ar-filled sealed glovebox in which all solutions were prepared and the incubation was performed. For the photoemission experiments, the samples were cleaned in the UHV system and were then extracted into air and transported in an Ar-filled or pumped out desiccator and inserted into the Ar atmosphere glovebox. The immersion times were between 2 and 30 min. This procedure follows the one used in experiments on sulfur adsorption from Na_2S solutions.[15] After the immersion the samples were rinsed with Milli-Q water in the glovebox and then dried under a stream of He or Ar before introducing into the UHV system.

Electrochemistry. A three-electrode electrochemical cell was employed using a mercury/mercuric oxide (MMO) and a platinum wire as reference and counter electrodes, respectively. All potentials in the text are referred to MMO. The base electrolyte, 0.1 M NaOH aqueous solution, was prepared with water of resistivity 18 MΩcm obtained from a Millipore purification system and solid analytical grade NaOH. Reductive electrodesorption of selenides from the substrates was performed at typically 0.05 V s^{-1} scan rate at 25 °C. In another set of experiments, voltammetry of Au electrode is carried out using 3 mM Na_2Se in aqueous 0.1 M NaOH solutions. Actual electrochemical area based on the roughness factor of the electrode was calculated from the charge associated with the gold oxide stripping peak in 0.5 M H_2SO_4. It is observed that the roughness factor was 1.56. The charges associated with the redox processes were determined for the actual electrochemical area after accounting for roughness factor.

Photoemission Measurements. The photoemission experiments have been performed in the UHV end-station of TEMPO beamline[47] at Synchrotron SOLEIL, where high resolution data have been recorded at different photon energies in the 60 to 800 eV range using a Scienta SES2002 electron spectrometer. Clean and ordered Au(111) and Ag(111) substrates were prepared by repeated cycles of Ar^+ sputtering and annealing at 800 K. The crystalline order and cleanliness of the samples were checked by LEED and by XPS, respectively. The high quality of the substrate surface was also checked by looking at the surface state band, which is well-known to be extremely sensitive to defects on the surface[48] and the observation here of narrow structures and a clear Rashba spin−orbit splitting proves the high quality of the clean substrate.

Measurements were made for a pass energy of 50 eV with an energy resolution better than 50 meV. In the following the binding energies in the XPS spectra are calibrated with respect to the Au($4f_{5/2}$) peak set at 84.0 eV.

RESULTS AND DISCUSSION

Selenium Adsorption on Au(111). *Electrochemistry.* Figure 1a shows the cyclic voltammograms in 0.1 M NaOH obtained after incubation of the Au surface in the Na_2Se solution for 30 min. The bulk electrolyte did not contain Na_2Se. The first cycle in the voltammograms show two clearly defined peaks, one at −0.86 V and another at −1.22 V in the cathodic direction for desorption processes and at −0.51 V in the anodic direction. The peaks observed in the positive potential of above 0 V are due to gold oxidation and the corresponding stripping process. The charge density after integration of peak at −0.86 V is 532 $\mu C/cm^2$. This is higher than the values of ∼200 $\mu C/cm^2$ reported for sulfur adsorption from Na_2S on gold.[13,17] The second peak at −1.22 yields values of 782 $\mu C/cm^2$ which is even higher that of the −0.86 peak. The second cycle does not show the peak at −0.86 while the one at −1.22 V reduces drastically with a small peak at −1.19 V. It is reported that there can be formation of atomic sulfur as well as polysulfide species when Na_2S is adsorbed on Au electrode.[17] Similar structures of Se have been reported[33] for Se formation on Au (from SeO_2 and H_2SO_4 solutions). It is likley that similar species based on selenium and polyselenide are

dx.doi.org/10.1021/jp4007203 | J. Phys. Chem. C 2013, 117, 9835−9842

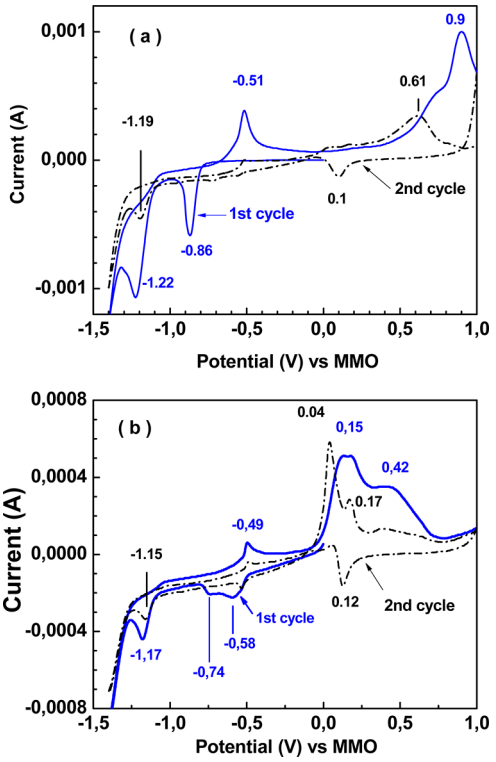

Figure 1. (a) Cyclic voltammograms in 0.1 M NaOH obtained at 50 mV/s scan rate, after incubation of the Au surface in the Na_2Se solution. The first and second scans are shown. (b) Voltammograms obtained at 50 mV/s scan rate in a cell with a 3 mM Na_2Se and 0.1 M NaOH aqueous solution.

formed on the Au surface in the present studies. This is supported by our XPS data as well, wherein atomic Se and Se_8 species are proposed, as described below. In the case of desorption of polymeric species, we deal with a situation where there would be interaction of Se atoms both with gold and within the polymeric species thus requiring higher desoprtion potential as opposed to Se chemisorption on Au. Furthermore the binding sites for the different atoms in the polymeric species can be different from the chemisorption case, also leading to more strongly bound species in the case of poymeric selenide. In such a case, one would expect higher charges associated with the desorption peaks and this is observed.

The peak observed at −0.51 V in the anodic direction is likely to be due to the readsorption of selenium species. The second cycle in the negative direction scanned after the formation of gold oxide and its stripping, does not show the peaks at −0.86 and −0.51 indicating that the gold surface is almost free from the selenium species. However, a small peak is observed at −1.19 V that may be due to the polymeric selenide present close to the surface. It is also suggested[17] that step edges are responsible for peaks observed at more negative potentials in case of sulfur adsorption[17] and this might be an additional reason for the observed higher charges as well and the residual peak in the second scan.

In the other set of measurements where the Au sample was immersed into the electrochemical cell containing 3 mM Na_2Se and 0.1 M NaOH aqueous solution, the voltammograms (Figure 1b) show a large peak at −1.17 V and two small peaks at −0.74 and −0.58 V. It is likely that the peak at −1.17 V is due to the polymeric selenide, while the peaks at −0.74 and −0.58 are for the selenium species on the Au surface. The important point to note is that the peak currents observed in this case are far smaller than those observed in the case of voltammograms wherein SAM formation has already taken place (Figure 1a). The charge associated with the peak at −1.17 (possibly the structure similar to the one observed at −1.22 V in the previous case) is 165 $\mu C/cm^2$ and is close to the reported values for similar systems.[13,17] The total charge for the two structures at −0.58 and −0.74 V is about 230 $\mu C/cm^2$, showing here a smaller intensity of the polymeric Se_8 form. In the case of the scan in Figure 1b, the Se adsorption occurs in less than 2 min. Hence, it is very likely that the time of contact between selenide solution and gold plays a role and possibly some catalytic chemical reactions result in a progressive formation of selenium and polyselenide species on the Au surface when it is exposed to the Na_2Se solution. Note that, based on XPS data, that Se_8 species is observed at all time scales investigated including 2 min immersion, although to a lesser extent, as discussed below.

Photoemission Measurements. An overview XPS spectrum for the clean Au(111) surface and after dipping into the Na_2Se solution for 2 min taken at 184 eV photon energy is shown in Figure 2 in the main region of interest here. The clean

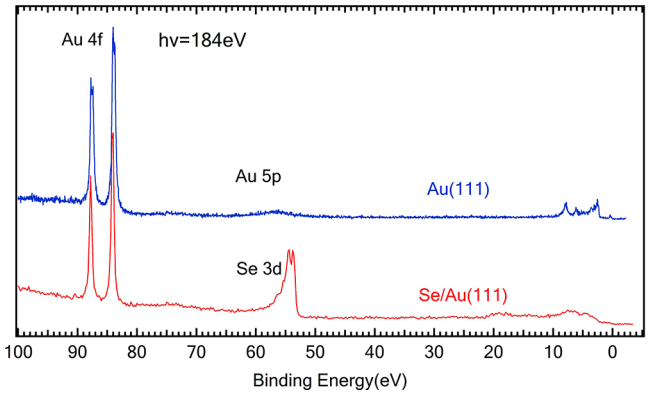

Figure 2. Overview XPS spectrum taken with a 184 eV photon energy for the clean Au(111) surface and after 2 min incubation in Na_2Se.

Au spectrum displays an intense doublet due to electrons photoemitted from the Au $4f_{7/2}$ (84 eV) and Au$4f_{5/2}$ levels (87.6 eV) and some other structures due to Au(5p) and the valence band (VB).

After incubation in the Na_2Se solution there appear pronounced structures with a binding energy of around 54 eV, related to Se atoms. Concurrently, changes in the valence band region can be noted. Note that the Se peak appears very intense at this low photon energy, because the Se(3d) excitation cross section is larger than for Au(4f). No structures at about 30 and 64 eV attributable to Na 2s and Na 2p, respectively, are observed. A possible problem could arise in this study because of the brief exposure of the Se exposed sample to air prior to insertion into the UHV chamber. As pointed out in the discussion of Se(3d) peak below, we did not, however, observe any signature of Se oxidation, which is known to produce a characteristical shift in Se binding energy.[21]

In Figure 3, the Au 4f spectra of the clean Au substrate and after Se adsorption are compared. The main component of the Au $4f_{7/2}$ peak at 84.0 eV is associated with bulk Au, whereas the shoulder at 83.7 eV is associated with the reconstruction of surface atoms of the Au surface as reported in literature.[49,50] The experimental spectrum was deconvoluted accordingly into

dx.doi.org/10.1021/jp4007203 | J. Phys. Chem. C 2013, 117, 9835−9842

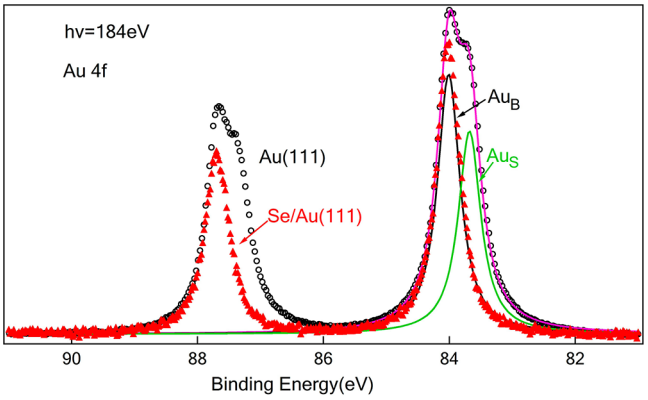

Figure 3. Au(4f) XPS spectra before and after Se adsorption as indicated. The lines Au_B and Au_S correspond to a deconvolution into bulk Au_B and surface Au_S components of the clean Au spectrum.

two components Au_B and Au_S as shown, using a Voigt line profile. After Se adsorption, the 83.7 eV shoulder disappears as a result of interaction with Se. This spectrum could be fitted with a Voigt profile with essentially the same parameters as the Au_B peak. By analogy with gold oxidation,[17] one could expect the appearance of a higher binding energy component if a gold selenide were formed, but this is not the case here. This shows that as previously noted for sulfur chemisorption in similar conditions (immersion in Na_2S aqueous solutions),[17] we deal with chemisorbed Se and not a gold selenide.

Changes in the VB region noted above in Figure 2 were investigated in more detail, using 60 and 184 eV photon energies. At higher energies closer to 200 eV the contribution of the 5d orbitals of gold is known to be significantly lowered.[51] Figure 4 shows the spectra for clean Au and after the 2 min

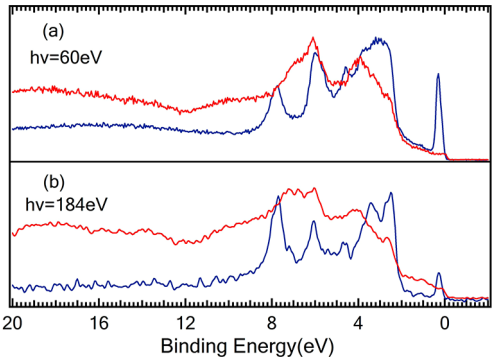

Figure 4. Valence band region for clean Au(111) (blue line) and after Se adsorption (red line) taken at two photon energies.

incubation. Se adsorption leads to the disappearance of the surface state peaks, near 0.45 eV and around 8 eV, probably due to the strong interaction of the Se molecules with the surface. On the other hand, Se leads to appearance of features due to bonding and antibonding states,[52] just above and below the Au d band region and the broad structures in the 12 to 20 eV region, due to Se(4p) and Se(4s) electrons. Also, changes in Au states because of interaction with Se are observed. We did not perform any calculations and there are no results known to us in the literature. On the other hand, it is known from earlier work[17] on the similar case of sulfur adsorption on Au that strong hybridization of the S 3s and 3p and Au valence states occurs, and somewhat similar features appear in calculations. As pointed out above and in the following, the Se adsorbed samples are exposed very briefly to air, but we did not observe oxidized Se species in XPS and, therefore, the changes in the spectra appear indeed assignable to Se. It should also be noted here that this spectrum contains contributions from different types of Se adsorption states as discussed below. Therefore, additional studies of direct adsorption of Se in UHV in submonolayer to multilayer conditions would be desirable in this context.

Finally, the XPS spectrum in the Se 3d region is reported in Figure 5, after Shirley background subtraction, for the case of 2

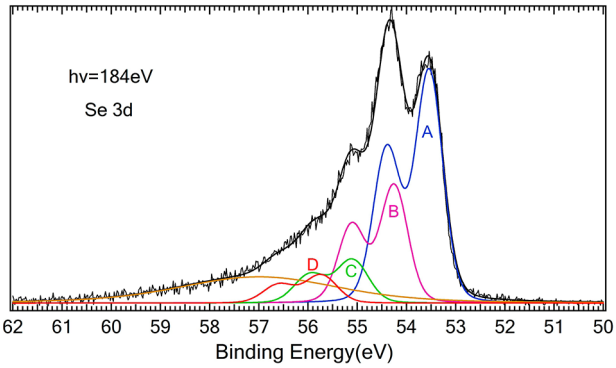

Figure 5. XPS spectrum in the Se 3d region. Curves correspond to deconvolution as described in the text. The broad yellow line centered at 57 eV is due to Au 5p, while the A–D doublets are attributed to Se, as discussed in the text.

min immersion. The spectra bear considerable resemblance to the ones observed for sulfur adsorption on Au[15,18] and were deconvoluted by analogy to these, assuming the existence of several components. These attributions are also consistent with earlier electrochemical STM imaging[33] that has shown that Se adsorption (in liquids) leads to a variety of structures: (a) a $(\sqrt{3} \times \sqrt{3})R30°$ structure with Se atoms in hollow sites[33] (see also calculations[27]), usually accompanied by (b) a square ring structure due to Se_8 as well as dimer, trimer, chain, and Se clusters.

Here we set Se doublet components with a 0.86 eV spin orbit splitting and a branching ratio of 0.66. The yellow line is due to a weak contribution from the broad Au(5p) structure[21,25] at 57.0 eV, seen in the clean Au spectrum. Note that no sharper doublet structure attributable to Se oxidation is observed at 57 eV.[21] The energy positions of the lower binding energy $3d_{5/2}$ doublet components are at 53.54 eV (A, blue), 54.25 eV (B, violet), 55.1 eV (C, green), and 55.73 eV (D, red). The different sets of doublets are attributed to (i) Se chemisorbed on gold atomically: blue doublet (A), (ii) a component due to polymeric Se_8 ring structures as reported in the literature from electrochemical STM measurement[33] and also seen for sulfur:[13,15] violet doublet (B), and (iii) two smaller components due to the other types of Se atoms (C, D): molecular and bulk-like components. The widths of peaks within the same doublet are set equal, but allowed to vary slightly between the first main pair of doublets (A, B; width 0.6 eV) and the second smaller intensity pair of doublets (C, D; width 0.7 eV). The larger width of the second pair of doublets could be due to actual existence of more components, which are unresolved here. In earlier lower resolution studies of evaporated[35] or electro-deposited[36] bulk-like Se deposits, binding energies of 55.3[35] and 55.48 eV[36] have been reported. To simulate only one bulk

dx.doi.org/10.1021/jp4007203 | J. Phys. Chem. C 2013, 117, 9835–9842

component, the spectrum could also have been fitted with just one component at 55.4 eV, instead of the C and D ones, but the width was much larger (1.1 eV), suggesting that this is in fact not the only component.

When the incubation time in the solution was increased from 2 to 10 min, the structure B attributable to polymeric Se_8 increased by about 20%, with respect to the A structure (see Supporting Information). This increase in the polymeric component with time is similar to reports for S adsorption.[17] The other components also increase. This observation appears consistent with temporal changes noted in the electrochemistry section above. They are also similar to observations on S adsorption.[17] A rough upper limit estimate of the Se layer effective thickness, derived assuming a homogeneous layer, gives a value of about 2.35 Å, as described in the Supporting Information. This suggests that, as for S,[17] we deal with a monolayer. In case of the 10 min spectrum, this effective thickness increases to about 3.35 Å, which must be due to the increase of the diversely packed Se_8 species, and the increase of the bulk-like component.

An investigation by LEED did not show any clear distinct features.

Selenium Adsorption on Ag(111). Incubation of Ag(111) in the Na_2Se solution even at the shortest times was observed to result in slight color change, resulting in a darker surface, as in photo toning.

In Figure 6a, the Ag XPS spectra of the clean Ag substrate are shown. The Ag binding energy was calibrated against the Au $4f_{7/2}$ one above at 84 eV and the Ag $3d_{5/2}$ peak position is found at 368.26 eV (Figure 6a), in agreement with high resolution XPS data in the literature.[54,55] Figure 6b shows the 60 eV binding energy region where a week structure due to Ag(4p) appears.

Upon Se adsorption, the plasmon structure at about 372 eV disappears and a very slight broadening (by 0.12 eV) toward lower binding energies of the Ag(3d) peaks occurs (Figure 6a). Changes in the VB region were noted and are reported in the Supporting Information (Figure 3). A deconvolution of the Ag(3d) peak was performed using two components corresponding to Ag and Ag interacting with Se (Ag_B and Ag_{Se}). First the XPS peak of clean Ag was accurately fitted using a Voigt profile (not shown here). The parameters of this fit were then used to define the shape of the Ag_B peak and allowing the Ag_{Se} peak position to vary. The results are shown in the inset in Figure 6a. The Ag_{Se} energy position in this fit is found to be 368.03 eV. It is lower than that of the clean Ag_B peak. This may appear somewhat strange from the point of view of the usual considerations based on the electrostatic potential model,[55] but is similar to the shifts observed for Ag oxidation[53,55] and sulfidation.[56] The shift appears somewhat smaller than for Ag oxidation, although in a recent study several oxidation states were reported corresponding to energy shifts from −0.23 eV to −0.9 eV.[55]

The spectrum in the Se(3d) region after incubation for 2 min is shown in Figure 7a where it is compared with the one for the

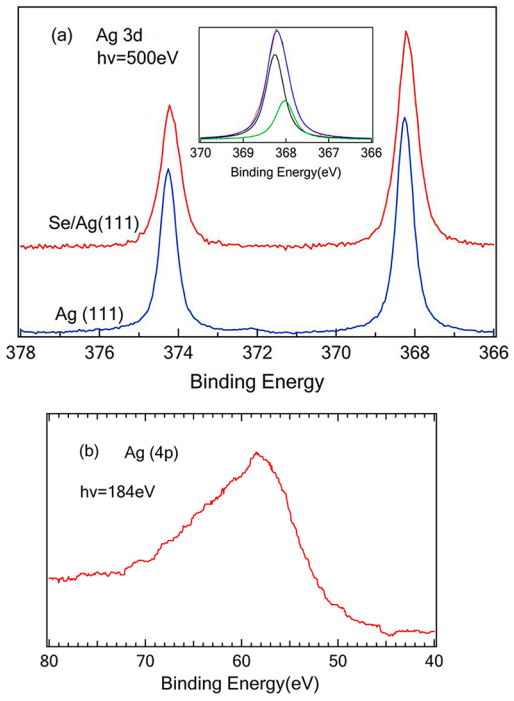

Figure 6. XPS spectra for (a) Ag(3d) prior to and after Se absorption. (b) Spectrum for clean Ag in the in the Se(3d) region showing structure due to Ag(4p). The inset in (a) shows deconvolution of the Ag peak with Se, into bulk Ag_B like (blue) and the smaller (green) selenide Ag_{Se} species (see text).

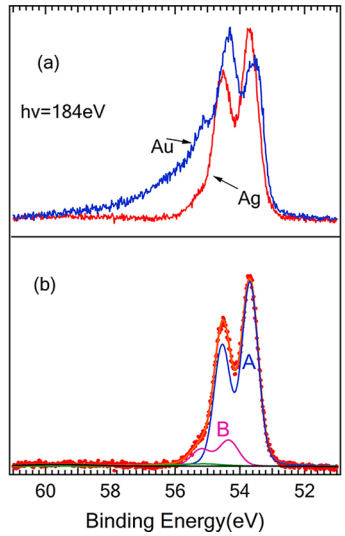

Figure 7. (a) Comparison of the spectra due to Se(3d) for the Ag and Au surfaces. (b) Deconvolution of the Se(3d) spectrum for the Ag surface is shown (see text).

Au surface. The Au and Ag spectra differ strongly in that the Ag spectrum is dominated by only one doublet component. In the case of Ag the first peak at the lower binding energy is positioned at a slightly higher binding energy than for Au. The existence of mainly these two structures in the spectra for Se(3d) on Ag are compatible with low resolution XPS data on Ag−Se films grown by successive Ag and Se deposition.[42]

After a Shirley background subtraction the spectrum was deconvoluted (Figure 7b) using the same widths and including a contribution from Ag, as determined from Figure 6b. In this fitting procedure we assume existence of mainly two components as for the main peaks in the Au case, since one can see a clear hump at about 55 eV. The energy positions of the first Se $3d_{5/2}$ doublet components are 53.68 eV (A) and 54.34 eV (B). An accurate fit requires inclusion of a third small

dx.doi.org/10.1021/jp4007203 | J. Phys. Chem. C 2013, 117, 9835−9842

Se component at 55.1 eV and the broad Ag(4p) structure located at 58.5 eV as may be seen in the clean Ag spectrum (Figure 6b). The contribution of the latter is however not significant. Again no clear structure attributable to Se oxidation is observed at 57 eV.[21]

In the case of Au(111) surface the 54.34 eV doublet B, was assigned to ring type structures of Se. In the Ag case the nature of the small feature B included at this energy in the above fit is unclear and more detailed microscopy studies are necessary to clarify this.

As for Au after the 2 min incubation no distinct LEED pattern was observed. However when subsequently removing Se in sputtering and annealing cycles we noted the appearance of a clear pattern, corresponding to a low coverage structure. This is given in the Supporting Information.

SUMMARY

In this paper, we presented results of a high resolution photoemission and electrochemistry study of Se adsorption on Au(111) and Ag(111) surfaces performed by immersion of pristine samples into an aquous solution of Na_2Se.

Cyclic voltammetry shows formation of selenium adsorbed species and structures observed in reductive desorption are related to the atomic and polymeric species noted in XPS. In case of the Au surface XPS spectra in the Se(3d) region in fact show two main features, that by analogy to what is known for sulfur and based on prior STM studies of Se adsorption on Au, we attribute to Se chemisorbed atomically and to polymeric Se_8 species. Some smaller features due to other species are also observed. The deconvolution of the Au(4f) XPS spectra also shows that we are not dealing with a gold selenide film. This is thus similar to the sulfur case. Note that recently a theoretical investigation[17] using DFT for sulfur adsorption, about the question of formation of S_8 rather than two-dimensional AuS, and where the experimental results are similar to ours, was performed. These calculations, which consider the evolution of the Au surface upon addition of S atoms do not indicate any displacement of Au atoms that would be necessary for formation of the sulfide and favor S_8 formation.

In case of adsorption on Ag(111) the XPS spectra for the Ag(3d) show a broadening of the peak to lower binding energies and a deconvolution into Ag_B bulk like and Ag_{Se} components shows that the Ag_{Se} is located at a 368.03 eV binding energy. This lower binding energy shift is similar to the case of oxidation and sulfidation of Ag. The Se(3d) XPS spectrum is found to be substantially different from the Au case and dominated by atomic Se corresponding to the selenide, though a smaller intensity, as yet unidentified Se structure at an energy similar to the polymeric Se_8 structure for Au, is also observed.

Investigation of the valence band region shows changes in Au/Ag states induced by Se adsorption. Se leads to appearance of features above and below the metal d band region attributable to hybridization of Se(4p) and Se(4s) and metal electrons. As pointed out in ref 17, the shape of projected DOS peaks could be used as a test of bonding or the type of molecules adsorbed. Calculations for different types of Se conformations on the surface would help to disentangle this information.

ASSOCIATED CONTENT

Supporting Information

Additional experimental results and complete ref list. This material is available free of charge via the Internet at http://pubs.acs.org.

AUTHOR INFORMATION

Corresponding Author

*E-mail: vladimir.esaulov@u-psud.fr.

Notes

The authors declare no competing financial interest.

ACKNOWLEDGMENTS

J.J. thanks the China Scholarship Council for supporting her Ph.D. work in France.

REFERENCES

(1) Love, J. C.; Estroff, L. A.; Kriebel, J. K.; Nuzzo, R. G.; Whitesides, G. M. Self-Assembled Monolayers of Thiolates on Metals as a Form of Nanotechnology. *Chem. Rev.* **2005**, *105*, 1103−1169.

(2) Schreiber, F. Structure and Growth of Self-Assembling Monolayers. *Prog. Surf. Sci.* **2000**, *65*, 151−257.

(3) Vericat, C.; Vela, M. E.; Benitez, G. A.; Carro, P.; Salvarezza, R. C. Self-Assembled Monolayers of Thiols and Dithiols on Gold: New Challenges for a Well-Known System. *Chem. Soc. Rev.* **2010**, *39*, 1805−1834.

(4) Guo, Z.; Zheng, W.; Hamoudi, H.; Dablemont, C.; Esaulov, V. A.; Bourguignon, B. On the Chain Length Dependence of CH_3 Vibrational Mode Relative Intensities in Sum Frequency Generation Spectra of Self Assembled Alkanethiols. *Surf. Sci.* **2008**, *602*, 3551−3559.

(5) Noh, J.; Kato, H. S.; Kawai, M.; Hara, M. Structural Transitions of Octanethiol Self-Assembled Monolayers on Gold Nanoplates after Mild Thermal Annealing. *J. Phys. Chem. B* **2006**, *110*, 2793−2797.

(6) Prato, M.; Moroni, R.; Bisio, F.; Rolandi, R.; Mattera, L.; Cavalleri, O.; Canepa, M. Optical Characterization of Thiolate Self-Assembled Monolayers on Au(111). *J. Phys. Chem. C* **2008**, *112*, 3899−3906.

(7) Hamoudi, H.; Guo, Z. A.; Prato, M.; Dablemont, C.; Zheng, W. Q.; Bourguignon, B.; Canepa, M.; Esaulov, V. A. On the Self Assembly of Short Chain Alkanedithiols. *Phys. Chem. Chem. Phys.* **2008**, *10*, 6836−6841.

(8) Millone, M. A. D.; Hamoudi, H.; Rodríguez, L. M.; Rubert, A.; Benitez, G. A.; Vela, M. E.; Salvarezza, R. C.; Gayone, J. E.; Sanchez, E. A.; Grizzi, O.; et al. Self-Assembly of Alkanedithiols on Au(111) from Solution: Effect of Chain Length and Self-Assembly Conditions. *Langmuir* **2009**, *25*, 12945−12953.

(9) Hamoudi, H.; Prato, M.; Dablemont, C.; Cavalleri, O.; Canepa, M.; Esaulov, V. A. Self-Assembly of 1,4-Benzenedimethanethiol Self-Assembled Monolayers on Gold. *Langmuir* **2010**, *26*, 7242−7247.

(10) García-Raya, D.; Madueño, R.; Blázquez, M.; Pineda, T. Formation of 1,8-Octanedithiol Mono- and Bilayers under Electrochemical Control. *J. Phys. Chem. C* **2010**, *114* (8), 3568−3574.

(11) Cometto, F. P.; Paredes-Olivera, P.; Macagno, V. A.; Patrito, E. M. Density Functional Theory Study of the Adsorption of Alkanethiols on Cu(111), Ag(111), and Au(111) in the Low and High Coverage Regimes. *J. Phys. Chem. B* **2005**, *109* (46), 21737−21748.

(12) Pensa, E.; Cortés, E.; Corthey, G.; Carro, P.; Vericat, C.; Fonticelli, M. H.; Benítez, G.; Rubert, A. A.; Salvarezza, R. C. The Chemistry of the Sulfur−Gold Interface: In Search of a Unified Model. *Acc. Chem. Res.* **2012**, *45* (8), 1183−1192.

(13) Gao, X.; Zhang, Y.; Weaver, M. J. Adsorption and Electrooxidative Pathways for Sulfide on Gold as Probed by Real-Time Surface-Enhanced Raman Spectroscopy. *Langmuir* **1992**, *8* (2), 668−672.

(14) McCarley, R. L.; Kim, Y.; Bard, A. J. Scanning Tunneling Microscopy and Quartz Crystal Microbalance Studies of Gold Exposed

to Sulfide, Thiocyanate, and *n*-Octadecanethiol. *J. Phys. Chem.* **1993**, *97*, 211−215.
(15) Vericat, C.; Vela, M. E.; Andreasen, G.; Salvarezza, R. C.; Vazquez, L.; Martın-Gago, J. A. Sulfur−Substrate Interactions in Spontaneously Formed Sulfur Adlayers on Au(111) *Langmuir 17*, 4919
(16) Yu, M.; Ascolani, H.; Zampieri, G.; Woodruff, D. P.; Satterley, C. J.; Jones, R. G.; Dhanak, V. R. The Structure of Atomic Sulfur Phases on Au(111). *J. Phys. Chem. C* **2007**, *111*, 10904−10914.
(17) Lustemberg, P. G.; Vericat, C.; Benitez, G. A.; Vela, M. E.; Tognalli, N.; Fainstein, A.; Martiarena, M. L.; Salvarezza, R. C. Spontaneously Formed Sulfur Adlayers on Gold in Electrolyte Solutions: Adsorbed Sulfur or Gold Sulfide? *J. Phys. Chem. C* **2008**, *112*, 11394−11402.
(18) Biener, M. M.; Biener, J.; Friend, C. M. Revisiting the S−Au(111) Interaction: Static or Dynamic? *Langmuir* **2005**, *21*, 1668−1671.
(19) Dishner, M. H.; Hemminger, J. C.; Feher, F. J. Scanning Tunneling Microscopy Characterization of Organoselenium Monolayers on Au(111). *Langmuir* **1997**, *13* (18), 4788−4790.
(20) Protsailo, L. V.; Fawcett, W. W. R. Electrochemical Characterization of the Alkaneselenol-Based SAMs on Au(111) Single Crystal Electrode. *Langmuir* **2002**, *18* (24), 9342−9349.
(21) Weidner, T.; Shaporenko, A.; Muller, J.; Schmid, M.; Cyganik, P.; Terfort, A.; Zharnikov, M. Effect of the Bending Potential on Molecular Arrangement in Alkaneselenolate Self-Assembled Monolayers. *J. Phys. Chem. C* **2008**, *112*, 12495−12506.
(22) Subramanian, S.; Sampath, S. Enhanced Stability of Short- and Long-Chain Diselenide Self-Assembled Monolayers on Gold Probed by Electrochemistry, Spectroscopy, and Microscopy. *J. Colloid Interface Sci.* **2007**, *312*, 413.
(23) Monnell, J. D.; Stapleton, J. J.; Jackiw, J. J.; Dunbar, T.; Reinerth, W. A.; Dirk, S. M.; Tour, J. M.; Allara, D. L.; Weiss, P. S. Effect of the Bending Potential on Molecular Arrangement in Alkaneselenolate Self-Assembled Monolayers. *J. Phys. Chem. B* **2004**, *108*, 9834−9841.
(24) Fonder, G.; Delhalle, J.; Mekhalif, Z. Exchange Versus Intercalation of n-Dodecanethiol Monolayers on Copper in the Presence of *n*-Dodecaneselenol and Vice Versa. *Appl. Surf. Sci.* **2010**, *256*, 2968−2973.
(25) Prato, M.; Toccafondi, C.; Maidecchi, G.; Chaudhari, V.; Nimbegondi, M.; Harish, K.; Sampath, S.; Parodi, R.; Esaulov, V. A.; Canepa, M. Mercury Segregation and Diselenide Self-Assembly on Gold. *J. Phys. Chem. C* **2012**, *116* (3), 2431−2437.
(26) Cometto, F. P.; Patrito, E. M.; Olivera, P. P.; Zampieri, G.; Ascolani, H. Electrochemical, High-Resolution Photoemission Spectroscopy and vdW-DFT Study of the Thermal Stability of Benzenethiol and Benzeneselenol Monolayers on Au(111). *Langmuir* **2012**, *28* (38), 13624−13635.
(27) Mankefors, S.; Grigoriev, A.; Wendin, G. Molecular Alligator Clips: a Theoretical Study of Adsorption of S, Se, and S−H on Au(111). *Nanotechnology* **2003**, *14*, 849−858.
(28) Suggs, D. W.; Stickney, J. L. Characterization of Atomic Layers of Tellurium Electrodeposited on the Low-Index Planes of Gold. *J. Phys. Chem.* **1991**, *95*, 10056−10064.
(29) Alanyalioglu, M.; Demir, U.; Shannon, C. Electrochemical Formation of Se Atomic Layers on Au(111) Surfaces: the Role of Adsorbed Selenate and Selenite. *J. Electroanal. Chem.* **2004**, *561*, 21−27.
(30) Zein, S.; Abedin, E.; Saad, A. Y.; Farag, H. K.; Borisenko, N.; Liu, Q. X.; Endres, F. Electrodeposition of Selenium, Indium, and Copper in an Air- and Water-Stable Ionic Liquid at Variable Temperatures. *Electrochim. Acta* **2007**, *52*, 2746−2754.
(31) Nagashima, S. Growth Modes of Se Overlayers Deposited on Au(111) Surfaces. *Appl. Surf. Sci.* **1997**, *121/122*, 116−119.
(32) Huang, B. M.; Lister, T. E.; Stickney, J. L. Se adlattices formed on Au(100), studies by LEED, AES, STM, and electrochemistry. *Surf. Sci.* **1997**, *392*, 27−43.
(33) Lister, T. E.; Stickney, J. L. Atomic Level Studies of Selenium Electrodeposition on Gold(111) and Gold(110). *J. Phys. Chem.* **1996**, *100*, 19568−19576.
(34) Cavallini, M.; Aloisi, G.; Guidelli, R. An in Situ STM Study of Selenium Electrodeposition on Ag(111). *Langmuir* **1999**, *15*, 2993−2995.
(35) Ouchi, A.; Bastl, Z.; Bohancek, J.; Orita, H.; Myazaki, K.; Miyashita, E.; Bezdicka, P.; Pola, J. Room-Temperature Reaction between Laser Chemical Vapor Deposited Selenium and Some Metals. *Chem. Mater.* **2004**, *16*, 3439−3445.
(36) Canava, B.; Vigneron, J.; Etcheberry, A.; Guillemoles, J. F.; Lincot, D. High Resolution XPS Studies of Se Chemistry of a Cu(In, Ga)Se_2 Surface. *Appl. Surf. Sci.* **2002**, *202*, 8−14.
(37) Sahu, A.; Qi, L.; Kang, M. S.; Deng, D.; Norris, D. J. Facile Synthesis of Silver Chalcogenide (Ag_2E; E = Se, S, Te) Semiconductor Nanocrystals. *J. Am. Chem. Soc.* **2011**, *133*, 6509−6512.
(38) Ferhat, M.; Nagao, J. Thermoelectric and Transport Properties of β-Ag_2Se Compounds. *J. Appl. Phys.* **2000**, *88*, 813.
(39) Chen, R.; Xu, D.; Guo, G.; Tang, Y. Electrodeposition of Silver Selenide Thin Films From Aqueous Solutions. *J. Mater. Chem.* **2002**, *12*, 1437−1441.
(40) Zhang, S.; Fang, C.; Wei, W.; Jin, B.; Tian, Y.; Shen, Y.; Yang, J.; Gao, H. J. Synthesis and Electrochemical Behavior of Crystalline Ag_2Se Nanotubes. *J. Phys. Chem. C* **2007**, *111*, 4168−4174.
(41) Xu, R.; Husmann, A.; Rosenbaum, T. F.; Saboungi, M. L.; Enderby, J. E.; Littlewood, P. B. Large Magnetoresistance in Nonmagnetic Silver Chalcogenides. *Nature* **1997**, *390*, 57.
(42) Chandra, B.; Mohanty, P. M.; Osipowicz, T.; Murty, B. S.; Varma, S.; Kasiviswanathan, S. Characterization of Silver Selenide Thin Films Grown on Cr-Covered Si Substrates. *Surf. Interface Anal.* **2009**, *41*, 170−178.
(43) Jiang, X.; Yu, A. Influence of Several Factors on the Growth of Selenium Nanowires Induced by Silver Nanoparticles. *J. Nanopart. Res.* **2008**, *10*, 475−486.
(44) Chen, X. F.; Hutchison, J. L.; Dobson, P. J. A One-Step Aqueous Synthetic Route to Extremely Small CdSe Nanoparticles. *J. Colloid Interface Sci.* **2008**, *319* (2008), 140−143.
(45) Neeraj; Rao, C. N. R. Metal Chalcogenide−Organic Nanostructured Composites from Self-Assembled Organic Amine Templates. *J. Mater. Chem.* **1998**, *8*, 279−280.
(46) Bertilsson, L.; Liedberg, B. Infrared Study of Thiol Monolayer Assemblies on Gold: Preparation, Characterization, and Functionalization of Mixed Monolayers. *Langmuir* **1993**, *9*, 141−149.
(47) Polack, F.; Silly, M.; Chauvet, C.; Lagarde, B.; Bergeard, N.; Izquierdo, M.; Chubar, O.; Krizmancic, D.; Ribbens, M.; Duval, J.-P.; et al. TEMPO: a New Insertion Device Beamline at SOLEIL for Time Resolved Photoelectron Spectroscopy Experiments on Solids and Interfaces. *AIP Conf. Proc.* **2010**, *1234*, 185−188.
(48) Forster, F.; Bendounan, A.; Ziroff, J.; Reinert, F. Systematic Studies on Surface Modifications by ARUPS on Shockley-Type Surface States. *Surf. Sci.* **2006**, *600*, 3870.
(49) Pasquali, L.; Terzi, F.; Seeber, R.; Nannarone, S.; Datta, D.; Dablemont, C.; Hamoudi, H.; Canepa, M.; Esaulov, V. A. UPS, XPS, and NEXAFS Study of Self-Assembly of Standing 1,4-Benzenedimethanethiol SAMs on Gold. *Langmuir* **2011**, *27* (8), 4713−4720.
(50) Pasquali, L.; Terzi, F.; Seeber, R.; Doyle, B. P.; Nannarone, S. Adsorption Geometry Variation of 1,4-Benzenedimethanethiol Self-Assembled Monolayers on Au(111) Grown from the Vapor Phase. *J. Chem. Phys.* **2008**, *128*, 134711.
(51) Duwez, A. S.; Di Paolo, S.; Ghijsen, J.; Riga, J.; Deleuze, M.; Delhalle, J. Surface Molecular Structure of Self-Assembled Alkanethiols Evidenced by UPS and Photoemission with Synchrotron Radiation. *J. Phys. Chem. B* **1997**, *101* (6), 884−890.
(52) Scheffler, M.; Stampfel, C. Theory of Adsorption on Metal Substrates. In *Handbook of Surface Science*; Horn, K., Scheffler, M., Eds.; Elsevier: New York, 2000; Vol 2, Chapter 5, p 285.
(53) Gao, X.; Wang, S.; Li, J.; Zheng, Y.; Zhang, R.; Zhou, P.; Yang, Y.; Chen, L. Study of Structure and Optical Properties of Silver Oxide

Films by Ellipsometry, XRD, and XPS Methods. *Thin Solid Films* **2004**, *455 −456*, 438−442.
(54) Frey, S.; Stadler, V.; Heister, K.; Eck, W.; Zharnikov, M.; Grunze, M.; Zeysing, B.; Terfort, A. Structure of Thioaromatic Self-Assembled Monolayers on Gold and Silver. *Langmuir* **2001**, *17* (8), 2408−2415.
(55) Gronbeck, H.; Klacar, S.; Martin, N. M.; Hellman, A.; Lundgren, E.; Andersen, J. N. Mechanism for Reversed Photoemission Core-Level Shifts of Oxidized Ag. *Phys. Rev. B* **2012**, *85*, 115445.
(56) Graedel, T. E.; Franey, J. P.; Gualtieri, G. J.; Kammlott, G. W.; Malm, D. L. On the Mechanism of Silver and Copper Sulfidation by Atmospheric H_2S and OCS. *Corros. Sci.* **1985**, *25*, 1163−1180.